ISSN 1330-3651 (Print), ISSN 1848-6339 (Online)
UDC/UDK 669.15.018.8:622.785

SINTERABILITY AND TENSILE PROPERTIES OF NICKEL FREE AUSTENITIC STAINLESS STEEL X15 CrMnMoN 17 11 3

Samir Butković

Original scientific paper
Nitrogen absorption during sintering of nickel free austenitic stainless steel X15CrMnMoN 17 11 3 changes its sinterability, affecting final dimensions, density, microstructure and tensile properties. Sinterability was analysed using alloy phase diagram combined with experimental results for linear shrinkage factor, density and microstructure. Tensile tests were performed using standard tensile tests specimens used in powder metallurgy (ISO 2740). The sintering was performed at 1200 °C and 1265 °C temperatures, in argon (Ar) and nitrogen (N_2) atmospheres, with the partial pressures between 400 mbar and 800 mbar. Sintering times between 3 h and 6 h were used. Lack of nitrogen, for parts sintered in argon atmosphere, resulted in final microstructure consisting of ferrite and austenite. Presence of ferrite during sintering caused better sinterability compared to parts sintered in nitrogen atmosphere, where austenitic microstructure was formed. It was found that increasing of nitrogen partial pressure causes strengthening of steel and increasing nitrogen content, while reduces density and shrinkage factor. Reduced ductility of steel after sintering was improved using solution annealing.

Keywords: *MIM technology, nickel free austenitic stainless steel, nitrogen, sintering*

Sinterabilnost i rastezna svojstva austenitnog čelika bez nikla otpornog na koroziju X15 CrMnMoN 17 11 3

Izvorni znanstveni članak
Apsorpcija dušika tijekom sinteriranja austenitnog čelika bez nikla otpornog na koroziju X15CrMnMoN 17 11 3 mijenja njegovu sinterabilnost, utječe na konačne dimenzije, gustoću, mikrostrukturu i rastezna svojstva. Sinterabilnost je analizirana pomoću faznog dijagrama legure u kombinaciji s eksperimentalnim rezultatima za faktor linearnog skupljanja, gustoću i mikrostrukturu. Rastezna ispitivanja provedena su na standardnim epruvetama za rastezna ispitivanja koje se koriste u metalurgiji praha (ISO 2740). Sinteriranje je provedeno na temperaturama 1200 °C i 1265 °C, u atmosferi argona (Ar) i dušika (N_2), s parcijalnim tlakom između 400 i 800 mbar. Rabljeno je vrijeme sinteriranja između 3 i 6 sati. Nedostatak dušika, za dijelove sinterirane u atmosferi argona, rezultirao je u konačnom mikrostrukturom koja se sastoji od ferita i austenita. Prisutnost ferita tijekom sinteriranja prouzročilo je bolju sinterabilnost u usporedbi s dijelovima sinteriranim u atmosferi dušika, gdje se formirala austenitna mikrostruktura. Utvrđeno je da povećanje parcijalnog tlaka dušika uzrokuje ojačanje čelika i povećanje sadržaja dušika, a smanjuje gustoću i faktor skupljanja. Smanjena duktilnost čelika nakon sinteriranja poboljšana je primjenom rastvarajućeg žarenja.

Ključne riječi: *austenitni čelik bez nikla otporan na koroziju, dušik, MIM tehnologija, sinteriranje*

1 Introduction

Allergic reactions caused by austenitic stainless steels containing nickel [1, 2], imposed development of new nickel free austenitic stainless steel produced by metal injection moulding process (Fig. 1). Lower price, compared to traditional austenitic stainless steels, makes this alloy very suitable for structural application [3]. Nitrogen, as a replacement for nickel, is absorbed from sintering atmosphere. Adding of nitrogen to the alloy in liquid state, due to reduced solubility, requires application of high pressure [4, 5]. However, since the solubility of nitrogen in austenite is much higher than in the liquid phase, the required amount of nitrogen in steel can be achieved through the absorption from the nitrogen containing sintering atmosphere [2]. Pre-alloyed ferritic steel powder is nitrided during sintering causing nickel equivalent increasing, resulting in austenitic microstructure (Fig. 1). Changing of microstructure at the sintering temperature makes this alloy specific for sintering. Densification and shrinking behaviour of alloy depend not only on temperature and time. In this case, fraction of phases at the sintering temperature is very important parameter affecting final properties of the steel.

Changes in chemical composition during nitrogen absorption cause changes in densification ability, shrinkage behaviour, microstructure and tensile properties of steel. In this regard, sinterability, microstructure, tensile properties and nitrogen absorption intensity of nickel-free austenitic stainless steel X15CrMnMoN 17 11 3 were analysed for different sintering conditions. Sinterability was investigated using alloy phase diagram, density and linear shrinkage factor results. Tensile tests were performed after sintering and solution annealing process to produce stress-strain curves.

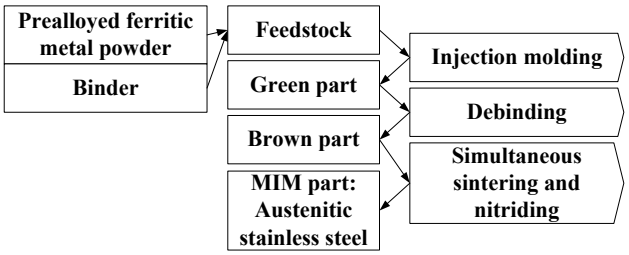

Figure 1 Injection moulding of prealloyed ferritic metal powder to produce austenitic stainless steel

During experimental work, sintering in argon atmosphere was performed first. In this case, original ferritic steel powder was sintered without significant changes in chemical composition.

Density, linear shrinkage factor, microstructure and tensile properties results were compared to those obtained using nitrogen containing sintering atmosphere, where increasing of nitrogen content occurs.

Debinding of injection moulded parts was done by catalytic debinding (CD 3045) method, while residual binder was debound using thermal debinding process. The sintering was performed in high temperature horizontal vacuum/hydrogen/inert atmosphere furnace MIM 3050.

2 Experimental work

2.1 Material

Nickel free prealloyed metal powder was mixed with appropriate binder to form feedstock. Lack of nickel in prealloyed metal powder, and reduction of nickel equivalent, resulted in ferritic microstructure. Chemical composition of powder is adjusted to improve nitrogen absorption during sintering. In this regard, manganese and molybdenum in this alloy primarily serve to increase the solubility of nitrogen in steel [4, 5, 6].

Typical chemical composition after sintering is presented in Tab. 1.

Table 1 Typical chemical composition of steel X15 CrMnMoN 17 11 3 after sintering

C /%	Cr /%	Ni /%	N /%	Mn /%	Mo /%	Fe
≤ 0,2	16,5 ÷ 17,5	≤ 0,1	0,75 ÷ 0,9	10 ÷ 12	3 ÷ 3,5	Rest

2.2 Injection moulding and catalytic debinding

Injection moulding of prepared feedstock was done in machine for injection moulding of metal powders type ALLROUNDER 320 C 600-100. The shape of the mould cavity corresponds to a standard specimen for tensile tests used in powder metallurgy (ISO 2740).

Debinding of injection moulded parts was done using catalytic debinding method. Polyacetal, as the main component of the feedstock, was decomposed by nitric acid HNO_3 [7, 8]. Parts were gradually heated to the temperature of 120 °C with preheating time of 30 min to equalize the temperature inside the furnace. Later, furnace remains at the temperature of 120 °C, blower, afterburner, nitrogen flow and nitric acid are switched on. Nitrogen flow rate of 50 l/min was used to spread nitric acid over the debinding furnace chamber. Nitric acid flow rate was 3,4 ml/min. Dwell time for catalytic debinding was 4 h, which is enough to decompose polyacetal from parts.

Backbone polymer, usually polyethylene, is included in the feedstock and remains after catalytic debinding to provide the necessary strength of brown part until the material starts to sinter [7, 8, 9]. Purging time of 30 min was used to remove residual acid to combustion chamber where it was burned by propane gas.

2.3 Thermal debinding and sintering

Thermal debinding and sintering were performed in the same furnace type MIM 3045. Parts were gradually heated to the temperature of 450 °C, using 3 °C/min heating rate. Dwell time at this temperature was 70 min, to insure uniform heating of parts. Degradation of residual binder begins at the temperature of 600 °C. Dwell time for thermal debinding was 2 h, which is enough for total removing of residual binder. Later, parts were heated to the temperature where mechanisms of sintering started to act. Thermal cycle of thermal debinding was the same for all experiments (Fig. 2). In order to have uniform heating of parts, heating of parts to the sintering temperature was performed in two segments. First, parts were heated to the temperature of 1050 °C, where dwell time of 45 min provided uniform temperature distribution through the parts. Next, parts were heated to the sintering temperature, where they were sintered to final density.

The sintering temperatures used in experiment were 1200 °C and 1265 °C. Sintering time levels were 3 h and 6 h, while the atmospheres used were argon and nitrogen. Also, partial pressures of nitrogen atmosphere were 400 mbar and 800 mbar.

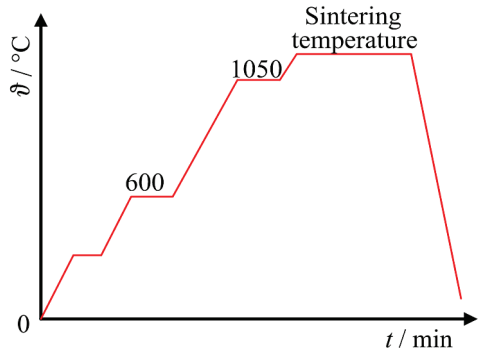

Figure 2 Thermal cycle of thermal debinding and sintering

Cooling of the sintered parts was done in two segments. First, parts were gradually cooled in MIM furnace to the temperature of 700 °C. Then, blower was turned on causing processing gas circulation around the parts resulting in faster cooling.

3 Results and discussion

3.1 Linear shrinkage factor and density

Linear shrinkage factor represents the shrinkage in one dimension of a compact during sintering. Determination of its value is essential for mould cavity dimensioning. Calculation of linear shrinkage factor was done using formula (1), measuring differences between the sintered and die dimensions [10, 11] (Fig. 3). Results are presented in the Tab. 2.

$$LSF, \% = \frac{\Delta L}{L_0} 100\,\%. \quad (1)$$

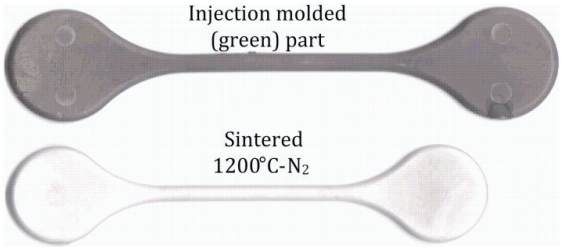

Figure 3 Comparison of injection moulded and sintered parts

Table 2 Sintering conditions, density and linear shrinkage factor results

Atmosphere	Temperature, °C	Time, h	Partial pressure, mbar	*LSF*, %	Density, g/cm^3
N_2	1200	3	400	12,9	7,33
Ar	1200	6	400	14,44	7,77
N_2	1200	6	400	13,77	7,59
N_2	1265	3	800	13,04	7,41
N_2	1200	3	800	12,68	7,31
Ar	1200	3	400	14,47	7,73

The density of the sintered parts was measured by Archimedes immersion method. Influential factors, their levels and average density for selected set of parameters are presented in the Tab. 2.

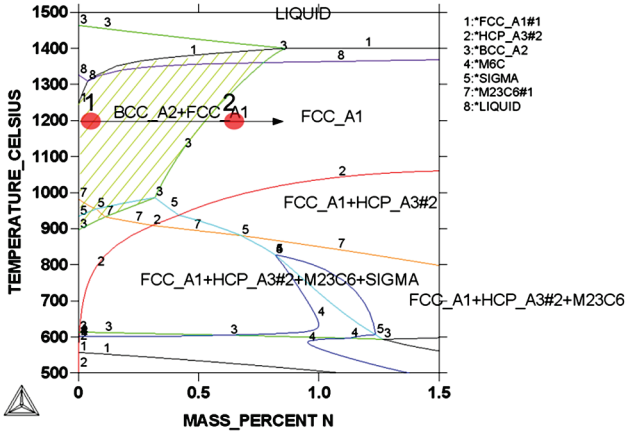

Figure 4 Computer generated phase diagram of alloy: 17 %Cr; 3 %Mo; 10 %Mn; 0,1 %C; Fe, N; Thermo-Calc Software

It was found that the sintering atmosphere has the strongest influence on density and linear shrinkage factor.

Sintering in argon atmosphere and the temperature of 1200 °C resulted in density of 7,73 g/cm^3 (Tab. 2). Linear shrinkage factor, in this case was 14,47 %. Sintering in nitrogen atmosphere, at the same temperature resulted in linear shrinkage of 12,9 % (Tab. 2) and decrease of density for about 5,4 %. Microstructures of polished samples (Fig. 5a,b) sintered in argon atmosphere reveal a significant lower percent of residual porosity compared to parts sintered in nitrogen atmosphere. Heating of prealloyed ferritic steel powder to the temperature of 1200 °C, brings alloy to region where austenite and ferrite exist (Fig. 4, point 1, shaded surface). Taking into account that diffusion rate of atoms in the body-cantered cubic (BCC) lattice is much greater as compared to the face-cantered cubic (FCC) lattice [10, 12], it can be concluded that sintering in this region increases overall diffusion coefficient, resulting in faster sintering and higher achieved densities.

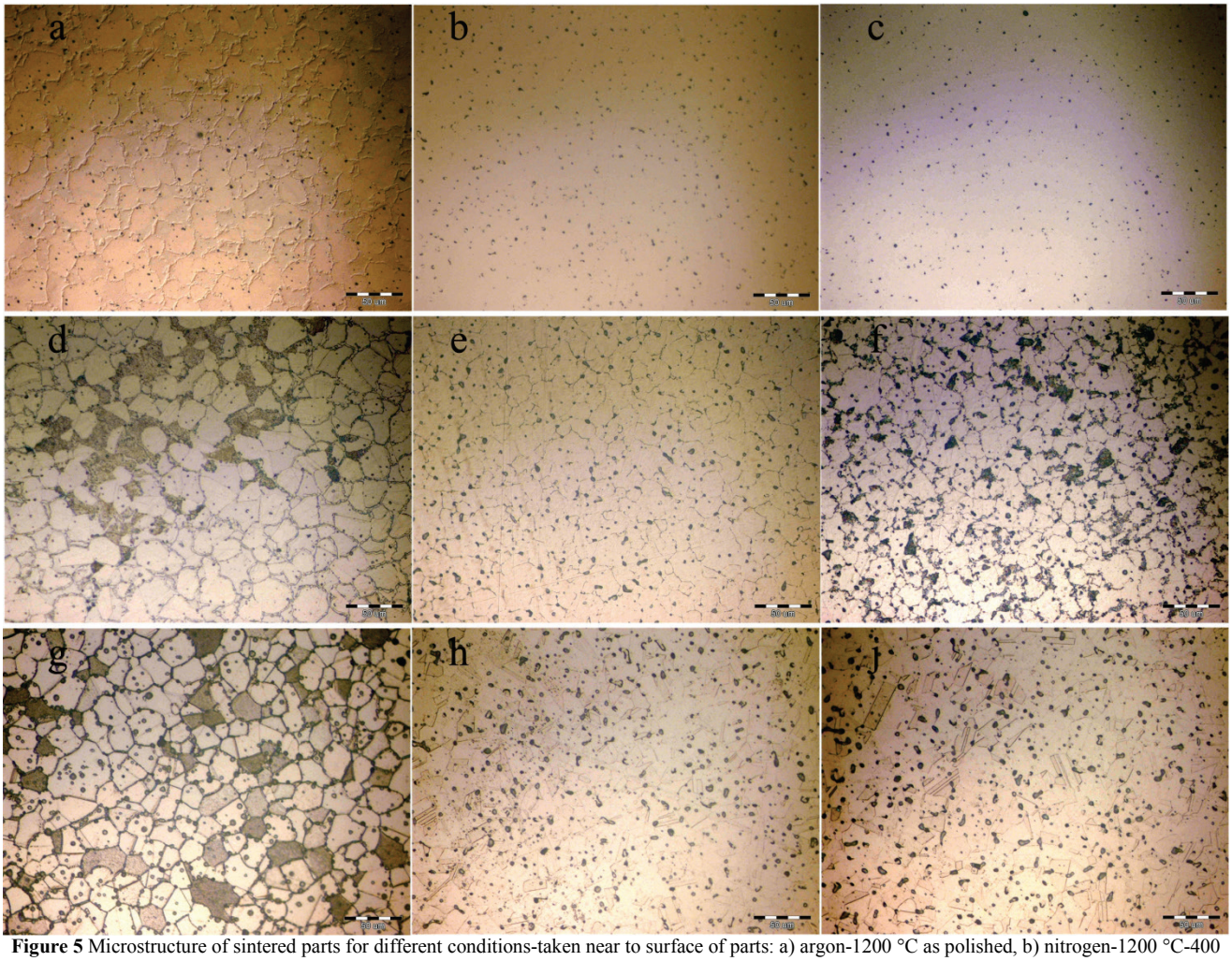

Figure 5 Microstructure of sintered parts for different conditions-taken near to surface of parts: a) argon-1200 °C as polished, b) nitrogen-1200 °C-400 mbar as polished, c) nitrogen1265 °C-800 mbar as polished, d) argon-1200 °C as etched, e) nitrogen-1200 °C-400 mbar as etched, f) nitrogen-1200 °C-800 mbar as etched, g) argon-1200 °C as etched-solution annealed, h) nitrogen-1200 °C-400 mbar as etched-solution annealed, j) nitrogen-1200 °C-800 mbar as etched-solution annealed

Also, nitrogen content after sintering in argon atmosphere was 0,0194 % (Tab. 3), causing nickel equivalent reduction. As a consequence, final microstructure of parts sintered in argon atmosphere consists of austenite and ferrite (Fig. 5 d,g, ferrite-dark regions). Sintering in nitrogen atmosphere causes change in chemical composition of alloy and increasing of nickel

equivalent (2). As a result, austenitic microstructure was formed (Fig. 5e).

$$Ni_{eq},\% = (Ni) + 0{,}5(Mn) + 0{,}3(Cu) + 25(N) + 30(C). \quad (2)$$

Absorbing of nitrogen during sintering (Tab. 3) moves alloy from region where austenite and ferrite exist to the point where only austenite exists (Fig. 4, point 2). Quantity of ferrite during sintering in nitrogen atmosphere (Fig. 4, point 1 to 2) decreases all the time, while austenitic phase grows. Reduced diffusion rate of atoms in austenite resulted in slower sintering, as well as reduced density and linear shrinkage of parts.

Nitrogen content for parts sintered in 400 mbar nitrogen atmosphere and the temperature of 1200 °C was 0,6145 % (Tab. 3). Raising of nitrogen partial pressure from 400 mbar to 800 mbar caused increasing of absorption intensity and final nitrogen content of 0,778 %. In this case, higher absorption rate accelerated transfer of alloy from the region where austenite and ferrite exist to the point where only austenite exists. In this case, linear shrinkage factor and density were reduced to 12,68 % and 7,31 g/cm^3 respectively (Tab. 2).

Table 3 Nitrogen content after sintering

Atm.	p / mbar	ϑ / °C	t / h	N / %
Ar	400	1200	3	0,0194
N_2	400	1200	3	0,614
N_2	800	1200	3	0,778
N_2	800	1265	3	0,693

Higher sintering temperatures caused more intensive atomic diffusion, faster sintering, reduction of residual porosity (Fig. 5c) and higher resulting density. Increasing of the sintering temperature from 1200 °C to 1265 °C, for the parts sintered in nitrogen atmosphere, resulted in average density increasing from 7,31 g/cm^3 to 7,41 g/cm^3. In this case, higher temperatures caused faster sintering, but also faster pore closing. The time for circulation of gas nitrogen through open pores is now reduced. The rest of the sintering time absorption of nitrogen was performed through surface of the parts. Also, higher temperature reduced [2-3] nitrogen solubility in austenite. As a consequence, raising of temperature from 1200 °C to 1265 °C caused reducing of nitrogen content in the steel from 0,778 % to 0,693 %.

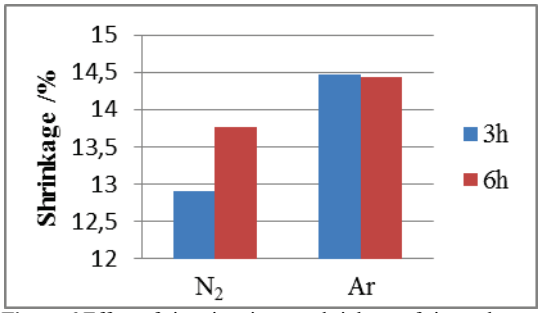

Figure 6 Effect of sintering time on shrinkage of sintered parts (1200 °C)

It is very important to notice that the density achieved at temperature of 1265 °C and nitrogen atmosphere (7,41 g/cm^3) is not even close to the density achieved at 1200 °C and argon atmosphere (7,73 g/cm^3).

This fact also emphasizes the importance of ferrite in microstructure at sintering temperature and its effect on sinterability.

Prolonged sintering time at the temperature of 1200 °C caused insignificant changes in density and linear shrinkage factor of the parts sintered in argon atmosphere (Tab. 2). However, increasing of sintering time to 6 h for the parts sintered in nitrogen atmosphere resulted in linear shrinkage factor increasing for about 6,7 %. This fact should be taken into consideration during tool cavity dimensioning and sintering parameters selection (Fig. 6).

3.2 Tensile properties

Tensile tests were done using Zwick machine. Results are presented in the form of stress/strain curves. The parts sintered in argon atmosphere, despite higher density have lower strength, yield strength and ductility. This behaviour is unusual for sintered materials where these factors are mostly dependable on sintered density [10]. Decisive influence in this case has the quantity of nitrogen absorbed during the sintering and achieved microstructure. The parts sintered in argon atmosphere have microstructure consisting of austenite and high quantity of ferrite which obviously has negative effect on mechanical properties (Fig. 7). Maximal strength and elongation achieved using argon atmosphere were 646 MPa and 10 % respectively. It was found that the tensile strength and elongation of the parts sintered in nitrogen atmosphere, where austenitic microstructure was formed, depend on its quantity and its form in steel (Figs. 8, 9 and 10). The parts sintered in 400 mbar nitrogen partial pressure and the temperature of 1200 °C experienced strengthening, with average strength of 802 MPa and elongation of 20 %.

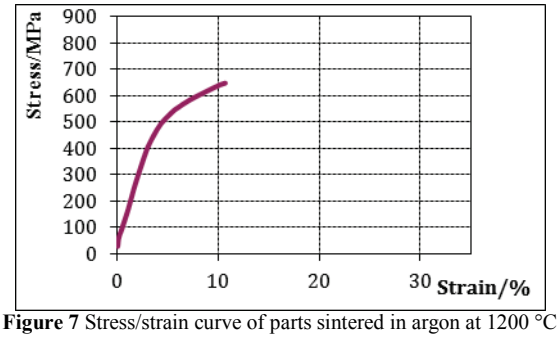

Figure 7 Stress/strain curve of parts sintered in argon at 1200 °C

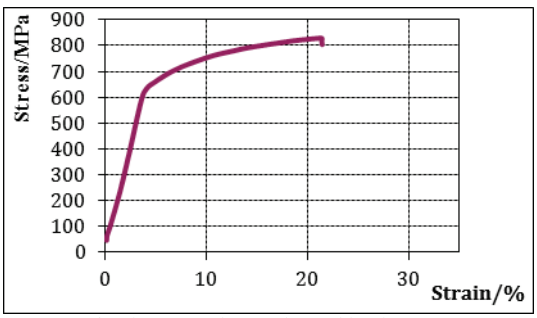

Figure 8 Stress/strain curve of parts sintered in nitrogen at 1200 °C and 400 mbar partial pressure

Increasing of nitrogen partial pressure to 800 mbar, where nitrogen content was increased (Tab. 3), caused more intensive strengthening of steel with 842 MPa of tensile strength (Fig. 9).

Precipitation of chromium nitrides during slow cooling of steel, after sintering, (Fig. 5 f, dark fields) caused reduction of its ductility. In this case, elongation was reduced to 12,5 %.

Improvement of ductility was observed on parts sintered at the temperature of 1265 °C. Reduction of residual porosity (Fig. 5c) and increased density contributed to better ductility of steel resulting in maximal achieved elongation of 29 % (Fig. 10). Increasing of the temperature and improvement of density did not significantly affect tensile strength, which is also unusual for the most traditional stainless steels [5, 6, 7, 10]. In this case, strength increasing by density was cancelled by reduced nitrogen content in steel (Tab. 3). Analysing presented stress/strain curves, it is obvious that the ductility achieved after sintering is significantly lower than the ductility of traditional austenitic stainless steel.

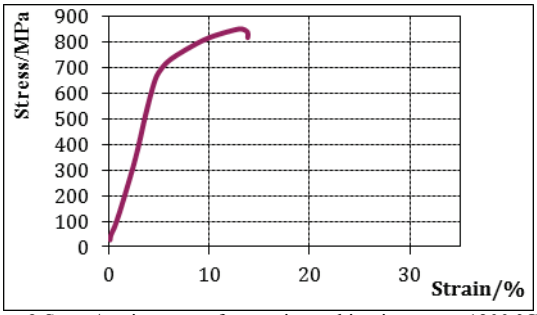

Figure 9 Stress/strain curve of parts sintered in nitrogen at 1200 °C and 800 mbar partial pressure

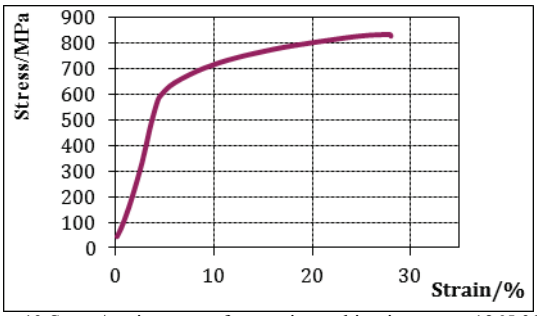

Figure 10 Stress/strain curve of parts sintered in nitrogen at 1265 °C and 800 mbar partial pressure

Precipitation of chromium nitrides formed during slow cooling after sintering appears as the main reason for this difference (Fig. 5 d). In order to remove nitrides formed after sintering and form fully austenitic microstructure solution annealing was performed. Computer generated phase diagram (Fig. 4) shows that full austenitic microstructure exists in region around 1150 °C. This temperature should provide dissolution of chromium nitride formed after sintering. Dwell time for solution annealing was 20 min, followed by water cooling. After solution annealing tensile tests were done. Large improvement of ductility can be observed on all samples solution annealed after sintering (Fig. 11). Metallographic examination showed clear austenitic microstructure without Cr_2N (Fig. 5 h, j). The elongation of the parts sintered in argon atmosphere was increased from 12 % to 35 %, at the same time, strength was not changed significantly (650 MPa) (Fig. 12).

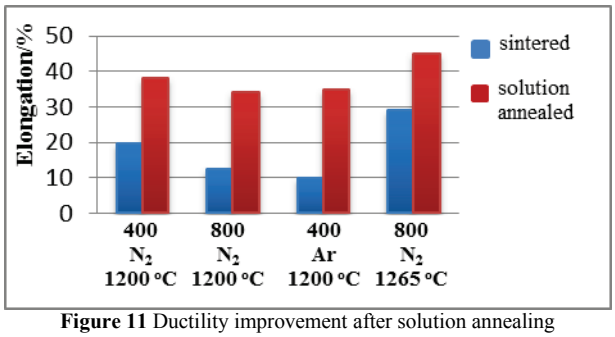

Figure 11 Ductility improvement after solution annealing

Strengthening by nitrogen is also evident after solution annealing. The maximal tensile strength of 820 MPa was achieved using 800 mbar nitrogen partial pressure and the temperature of 1200 °C. Reducing of partial pressure from 800 mbar to 400 mbar, for parts sintered at 1200 °C, resulted in increasing of elongation from 33 % to 38 %, while strength was reduced for about 5 % (Figs. 13, 14).

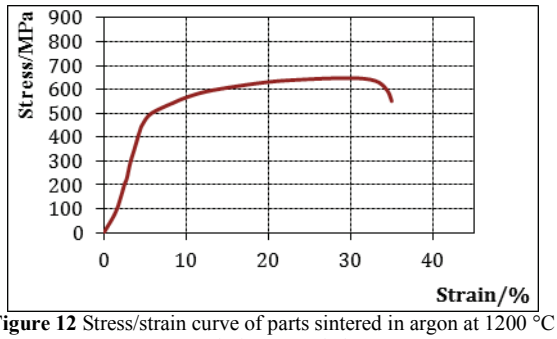

Figure 12 Stress/strain curve of parts sintered in argon at 1200 °C (solution annealed)

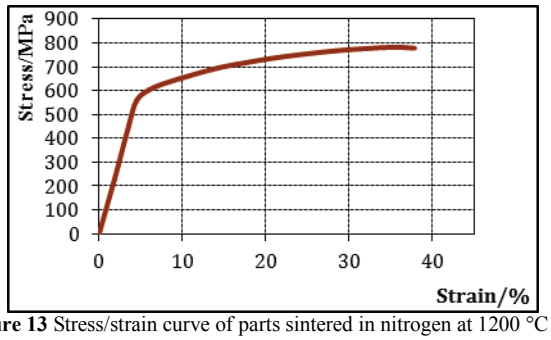

Figure 13 Stress/strain curve of parts sintered in nitrogen at 1200 °C and 400 mbar partial pressure (solution annealed)

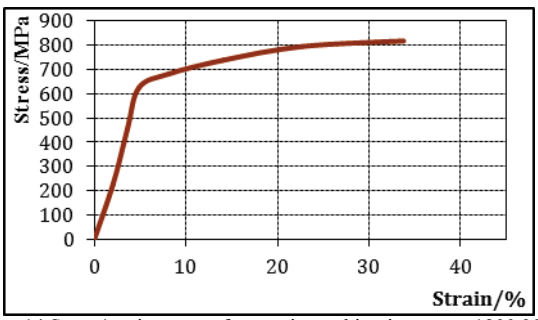

Figure 14 Stress/strain curve of parts sintered in nitrogen at 1200 °C and 800 mbar partial pressure (solution annealed)

The best ductility was achieved using the temperature of 1265 °C and 800 mbar nitrogen partial pressure. In this case, solution annealing caused increasing of the elongation from 29 % to 45 % (Figs. 11, 15) and reducing of strength from 833 MPa to 795 MPa.

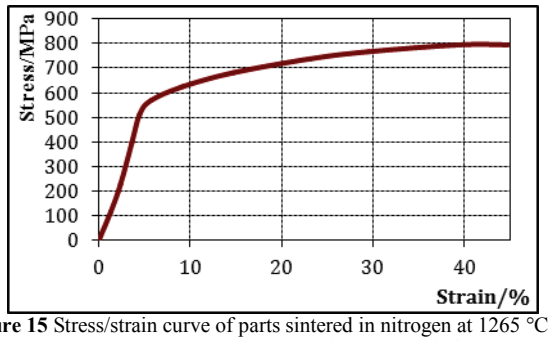

Figure 15 Stress/strain curve of parts sintered in nitrogen at 1265 °C and 800 mbar partial pressure (solution annealed)

Generally, it can be noted that solution annealing resulted in remarkable elongation increasing. More than 50 % increasing of elongation was achieved after solution annealing for all experiment. Reduction of strength can be observed, but negligible compared to the elongation increasing.

Solid solution strengthening with nitrogen caused strength and yield point higher than in traditional austenitic stainless steel. This fact should be considered during MIM material selections.

4 Conclusion

Sinterability of nickel free austenitic stainless steel X15CrMnMoN 17 11 3, compared to traditional austenitic stainless steels, does not depend only on sintering parameters, but also on crystal structure and phase ratio at the sintering temperature [13]. Lack of nitrogen in the parts sintered in argon atmosphere resulted in microstructure consisting of austenite and ferrite. Presence of ferrite at the sintering temperature of 1200 °C caused faster sintering with higher density and shrinkage factor.

Introducing of nitrogen in process changes chemical composition of alloy during sintering, resulting in formation of fully austenitic microstructure. Higher partial pressure of nitrogen causes increasing of its absorption rate during sintering. Nitrogen percent absorbed during sintering at the temperature of 1200 °C and partial pressure of 400 mbar was 0,614 %, while sintering in 800 mbar nitrogen partial pressure resulted in nitrogen percent of 0,778 %. Increasing of the sintering temperature resulted in increased density and improved mechanical properties of sintered parts, while nitrogen absorption rate was decreased. Reduced density, compared to parts sintered in argon atmosphere did not affect significantly mechanical properties.

Strengthening of the alloy was observed as nitrogen percent increased [13]. Maximal strength of 842 MPa was achieved using 800 mbar nitrogen atmosphere and the temperature of 1200 °C. Also, increasing of nitrogen content in steel resulted in precipitation of chromium nitride leading to large reduction of elongation. Maximal elongation of 28 % for parts sintered at 800 mbar nitrogen partial pressure and the temperature of 1265 °C, was observed.

Reduction of Cr_2N formed during slow cooling after sintering resulted in slight reduction of tensile strength but large increase of ductility of steel. Maximal achieved elongation of 45 % was observed for parts sintered at the temperature of 1265 °C and 800 mbar nitrogen partial pressure.

5 References

[1] Winters, G. L.; Nutt, M. J. Stainless Steels for Medical and Surgical Applications, West Conshohocken, ASTM International, 2002.
[2] Schino, A. D. I.; Kenny, J. M. Development of high nitrogen, low nickel 18 %Cr, austenitic stainless steel. // Journal of material science, 35(2000), pp. 4803-4808.
[3] Kerr, J.; Paton, R. Preliminary investigations of low-nickel stainless steels for structural applications. // Tenth International Ferroalloys Congress, Cape Town, South Africa, 2004, pp. 757-765.
[4] Iorio, L.; Cortie, M.; Jones, R. Solubility of nitrogen in experimental low-nickel austenitic stainless steel. // The Journal of The South African Institute of Mining and Metallurgy, July 1994, pp.173-190.
[5] Speidel, M. O. Nitrogen Containing Austenitic Stainless Steels. // Mat-wiss. u. Werkstofftech. 37(2006), pp. 875-880.
[6] Pistorius, P. C.; du Toit, M. Low-nickel austenitic stainless steels: metallurgical constraints. // The Twelfth International Ferroalloys Congress Sustainable Future, Helsinki, Finland, 2010, pp. 911-918.
[7] Aude-Porter, M. Effect of binder system for Metal Injection Molding, Master thesis, Lulea University of Technology, 2003.
[8] German, R. M. Injection Molding of Metals and Ceramics, New Jersey, 1997.
[9] ASM Handbook: Powder Metal Technologies and Applications, Volume 7, 1998.
[10] Klark, E.; Samal, P. K. Powder Metallurgy Stainless Steels, USA 2007.
[11] Randall M. German; Sintering theory and practice, New York, 1996.
[12] Rassmus, J.; Larsson, A.; Grosser, H. An approach to cost effective low alloyed materials for MIM. // PIM International, 5, 3(2011), pp. 78-82.
[13] Butković, S. Uticaj parametara sinterovanja na osobine dijelova od modificiranih nehrđajućih čelika dobivenih MIM tehnologijom, Doktorska disertacija, University of Tuzla, 2011.

Authors' adresses

Dr. sc. Samir Butković
Mašinski fakultet Tuzla
Univerzitetska 4, 75000 Tuzla
Bosnia and Herzegovina
Tel.: 0038761391753
E-mail: samir.butkovic@untz.ba